Mining
Mineração

Development of innovation routes for iron ore using high intensity magnetic separators

http://dx.doi.org/10.1590/0370-44672021750076

Késsius Bortolan Menezes[1,3]
https://orcid.org/0000-0002-1204-4567
Ana Vitória de Moura Gonçalves[2,4]
https://orcid.org/0000-0002-5609-8786
Otávia Martins Silva Rodrigues[2,5]
https://orcid.org/0000-0003-2328-5398
Érica Linhares Reis[2,6]
https://orcid.org/0000-0003-3760-9904

[1]Centro de Tecnologia Mineral, Anglo American, Conceição do Mato Dentro - Minas Gerais - Brasil.

[2]Universidade Federal de Ouro Preto - UFOP, Escola de Minas - Departamento de Engenharia de Minas, Ouro Preto - Minas Gerais - Brasil.

E-mails: [3]kessius.menezes@angloamerican.com, [4]ana.moura@aluno.ufop.edu.br, [5]otaviarodrigues@ufop.edu.br, [6]erica@ufop.edu.br

Abstract

The mineral processing of low-grade iron ores commonly generates large volumes of slime, which are disposed as tailings. Modern mining requires strives to eliminate the use of tailings dams in a maximum effort to increase metallurgical recovery, the security and reduction of the operational cost. This research aims for the recovery of iron contained in the slime, which consists of a material with 38% Fe and <40 µm, originating from the desliming cyclones. Pilot tests were performed on the Wet High-Intensity Magnetic Separator (WHIMS) and on the Vertical Ring Pulsating High Gradient Magnetic Separator (VPHGMS) considering different configurations in terms of operating parameters and routes. The best results were obtained for VPHGMS with an iron content in the concentrate of 67.06% and mass and metallurgical recovery of 32.42% and 56.86%, respectively. In the best condition tested, around 540 thousand tons of concentrate can be incorporated into production and has great environmental relevance.

Keywords: iron ore, slime ultrafines, high-intensity magnetic separator, dispersion, processing routes.

1. Introduction

Maximizing profit and minimizing costs are necessary actions, however the main goal is to reduce the environmental impacts. Thus, the reprocessing of tailings is essential (Li *et al*., 2010; Wolff & Dutra, 2010; Roy & Das, 2013; Jena *et al*., 2015; Ozcan & Celik, 2016; Mohanty *et al*., 2017; Ribeiro *et al*., 2017; Dauce *et al*., 2019; Rocha *et al*., 2019). Turning the tailings or part of them into assets has been a great current challenge because there is still a lack of economically viable technologies in the mining industry for the recovery of the material of interest present in the tailings from the processing of iron ore.

The tailings of the industrial desliming stage have been the focus of many studies, since this material can reach up to 20% of the ROM (Run of Mine) in the beneficiation plants and has an iron content similar to the ROM. The slime contains a high percentage of particles smaller than 10 µm and a complex mineralogy. Thus, it is not easy to discover and use a suitable and economically viable method for a stage of concentration of this type of material (Wolff & Dutra, 2010; Jena *et al*., 2015; Ozcan & Celik, 2016; Roy & Das, 2013; Mohanty *et al*. 2017; Ribeiro *et al*., 2017; Dauce *et al*., 2019; Rocha *et al*., 2019).

The use of high-intensity magnetic separators for concentration of low-grade iron ores and tailings from processing plants has proved to be an advantageous technique. This process addresses the economic, environmental, and strategic issues of mining, allowing the recovery of iron from tailings and reduces the environmental impacts (Forssberg & Kostkevicius, 1982; Silva & Luz, 2003; Svoboda & Fujita, 2003;

Li *et al.*, 2010; Mohanty *et al.*, 2017; Wolff & Dutra, 2010; Yanga, *et al.*, 2011; Ribeiro *et al.*, 2017; Rocha *et al.*, 2019).

Studies have been carried out considering the application of WHIMS for the recovery of iron oxides contained in tailings and slime from the processing of iron ore. Promising results could be observed even for tailings with an iron content between 23% and 34% and with particle size distribution (PSD) below 10 µm (Wang & Forssberg, 1994; Silva & Luz, 2003; Arol & Avdogan, 2004; Chen *et al.*, 2009; Dworzanowski, 2014; Jena *et al.*, 2015; Ribeiro *et al.*, 2017; Rocha *et al.*, 2019).

The vertical pulsating high gradient magnetic separator (VPHGMS) is one alternative to WHIMS. In addition to the magnetic field and the matrix system, the former uses a pulsating medium and gravity to benefit fines for weakly magnetic minerals. It has high efficiency and a low operating cost. Both machines, however, work better for materials with between 0.01 mm and 1.0 mm. The main difference between the VPHGMS and WHIMS is the matrix system, which highlights the clogging problems of the WHIMS separators and the matrix system associated with the VPHGMS pulsating (Zeng & Dahne, 2003; Chen *et al.*, 2009).

Dispersants have been used as an alternative for magnetic separation processes that are impaired by the aggregation of non-magnetic particles and magnetic particles, which prevents them from being separated when exposed to a field induced by the equipment. Another issue is the fine particles that tend to aggregate or cover other coarser particles. A step prior to concentration in order to disperse the material can increase the chance of recovery of the particle with magnetic susceptibility (Song *et al.*, 2002; Lu *et al.*, 2005; Martinez *et al.*, 2011).

In this context, magnetic concentration tests using high intensity magnetic separators are proposed in this study, in order to evaluate their operation as a concentration step for slime in the processing of iron ore from a beneficiation plant in Minas Gerais, Brazil. This is expected to increase the metallurgical recovery of the process, in addition to generating a lower amount of material to be disposed.

2. Material and method

2.1 Characterization studies

Sampling of the slime tailings pulp with 5% solids was performed in order to obtain a consistent mass to perform the characterization, and also to test the different concentration routes using the magnetic separators.

The particle size distribution analysis was performed by a laser granulometer model Saturn Digisizer II from Micromeritics. The mineralogical characterization of the slime was performed using a scanning electron microscope (SEM) automated with the QEMSCAN® system with a tungsten source model EVO-50 from Zeiss. The iMeasure software was used to perform the measurements and the data were processed using the iDiscovery software. The QEMSCAN® was operated using a voltage acceleration of 25 kV and a current of approximately 5 nA.

The major chemical elements and/or compounds of the slime were quantified by the analytical method of x-ray fluorescence in fused tablets, using the Axios Fast device from Panalytical. The stoichiometric closure considers the loss on ignition (LOI). Weighing the sample before and after fusion helps to determine the total LOI.

2.2 Technological studies

Different routes were proposed for the technological study using WHIMS (Wet High Intensity Magnetic Separation) and VPHGMS (Vertically Ring Pulsating High Gradient Magnetic Separation), both pilot scale equipment.

All magnetic separation tests using WHIMS were performed using the Minimag high-intensity magnetic separator, model G-340, from the GAUSTEC, with a feed capacity of 288 kg/h. A rotation of 5 rpm, concentrate wash pressure at 4.0 kgf/cm² and volumetric feed flow at 0.46 m³/h were used. The magnetic separation tests using the VPHGMS, were performed using the Slon® magnetic separator, from Outotec, model 750, with a feed capacity of 250 kg/h. All tests were performed considering the parameters set for the rotation of 2 rpm, volumetric feed flow at 0.54 m³/h and the pulse can be set to 300 pulses/minute.

2.2.1 Route 1: Magnetic separation using natural desliming tailings (WHIMS)

A factorial experimental design was performed in order to investigate the influence of the magnetic field, the matrix and percentage of solids in the feed pulp. The analyzed responses were iron content in the concentrate, mass and metallurgical recovery. The experiment sought to manipulate the controllable factors and analyze their respective effects on the process outputs. Thus, the process variables that were actually considered in the planning and optimization of the experiment are summarized in the Table 1.

Table 1 - Approach to performed experimental design.

Controllable Input Factors	x_1 = Magnetic Field (T)	[1.2; 1.6]
	x_2 = Matrix (mm)	[0.5; 1.1; 1.5]
	x_3 = Solids (%)	[5; 20; 36]
Outputs	y_1 = Mass Recovery (%)	[0; 100]
	y_2 = Metallurgical Recovery (%)	[0; 100]
	y_3 = Iron Content (%)	[38; 70]

From the simulated experimental data, it was possible to draw conclusions about the influence of controllable factors on the process outputs. This analysis was performed in Minitab® software. Thus, it was possible to optimize the experiment's responses through a Minitab® tool accessed in the Stat / DOE / Factorial / Response Optimizer options. The "Response Optimizer" tool made it possible to identify the best options for the process, and also the expected results or changes that should be made in the event of a change in the condition of any of the optimal factors.

2.2.2 Route 2: Magnetic separation preceded by dispersion (WHIMS)

The magnetic separation tests for this stage were performed considering the best configuration obtained in Route 1 in terms of magnetic field, matrix and percentage of solids. Dispersion tests, for the desliming tailing pulp, were also performed preliminarily for this route, and the best dispersion results were obtained for sodium silicate.

Zeta potential (ZP) measurements were performed in order to explain the benefit of dispersion with sodium silicate. The zeta potential measurements were performed using a Zetasizer nano. Pure hand samples (hematite, quartz and goethite) were collected in the mine region. The samples were milled using an agate mortar and pestle. Mineral suspensions of 0.1% (w/w) were prepared with particles size of below 38 µm at the absence and presence of dispersant (sodium silicate - 10mg/L). NaCl solution, $1x10^{-4}$ mol/L, was used as the indifferent electrolyte. HCl solution of 0.5% (v/v) and a NaOH solution of 0.5% (w/v) were used as pH modifiers. The pH values were adjusted between 9 and 11 to measurement the zeta potential.

2.2.3 Route 3: Magnetic separation preceded by dispersion and an additional desliming step (WHIMS)

The magnetic separation tests for this stage were performed considering an additional desliming step before the magnetic concentration. The additional desliming was performed using a pilot scale hydrocyclone with a diameter of 2.0 inches. The feed from the additional desliming step contained a pulp with 5% solids. In 50% of the passes (d_{50}), the particle size of the additional desliming was 17 µm for the result corrected by the Plitt equation. In this route, the same operational conditions as employed previously, i.e. using the best operational configuration obtained in Route 1 for magnetic concentration and the same dispersing reagent under the same conditions in the Route 2 were applied. The experimental design was carried out in Minitab 18® software in order to obtain the best optimization conditions for tests. The tests were performed, at least, in duplicate.

2.2.4 Route 4: Magnetic separation preceded by dispersion (VPHGMS)

For these tests, a factorial experiment was designed using the Minitab 18® software. The magnetic separation tests for this last stage were performed considering magnetic field at a 1 T, matrix of 1.5 mm and pulsation of 300 pulses per minute. These parameters were selected based on bench tests previously performed on the Slon model 100 equipment. In these bench tests, a factorial experimental design was carried out using a magnetic field between 0.8 T and 1 T, matrix opening of 1.5 mm and 2.0 mm and pulse rate of 300 pulses per minute and 400 pulses per minute.

3. Results and discussion

3.1 Characterization studies

In the sample used for this study, 87.15% was below 38 µm and 42.41% was below 10 µm. Sieving produced a size of 28 µm for 80% of the mass (d_{80}). The tailings had 38.08% of Fe, 33.67% of SiO_2 and 5.92% of Al_2O_3. The mineralogical study showed mainly hematite, goethite, quartz, muscovite, kaolinite and gibbsite. Hematite and clay minerals are the predominant mineral species smaller than 20 µm granulation. Almost 60% of quartz is also below 20 µm and about 40% is between 20 µm and 80 µm (see Table 2).

Table 2 - Quantity (%) of the major mineral species of the desliming tailing distributed by granulometry intervals. Automated scanning electron microscope with the QEMSCAN® system with Zeiss model EVO-50 tungsten source.

Range (µm)	Hematite	Quartz	Caulinite	Muscovite	Goethite	Gibbsite
0-20	96.7	58.2	93.1	92.5	87.1	98.1
20-40	3.3	26.4	5.9	6.7	8.6	1.4
40-80	0.0	13.9	1.0	0.8	4.1	0.6
80-160	0.0	0.3	0.0	0.0	0.1	0.0
160-320	0.0	1.2	0.0	0.0	0.0	0.0
Total	**100.0**	**100.0**	**100.0**	**100.0**	**100.0**	**100.0**

According to photomicrograph (Figure 1), abundant presence of hematite and goethite associations were observed. This goethite presence is generally classified as earthy goethite, that is, it has a higher degree of hydration and earthy consistency, with very fine granulometry (less than 10 µm) and higher contaminants. For the other mineral phases (quartz and clay minerals), few associations were observed.

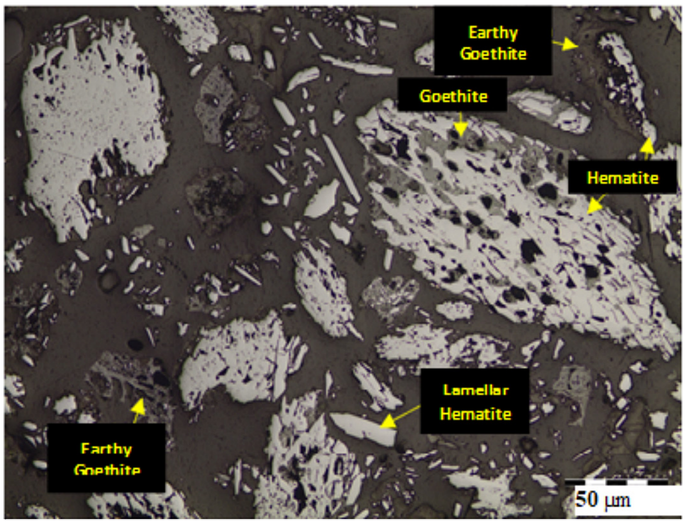

Figure 1 - Hematite + goethite association. Photomicrograph. Reflected light, parallel nicols.

3.2 Technological studies

3.2.1 Route 1

An experimental design was carried out in Minitab 18® software in order to obtain the best optimization conditions for the following tests. In this experimental design, the input variables were matrix opening, magnetic field and percentage of solids. The output variables were iron content in the concentrate, mass recovery and metallurgical recovery.

The maximized value was expected for all output variables. Thus, it was possible to obtain the highest value for parameter D (desirability) as a function of the output variables. The result showed that the optimal condition for the adopted premise would be the operation with 0.5 mm matrices, 1.6 T magnetic field and 5% solids percentage (Figure 2).

The optimized results for mass recovery, iron content in the concentrate and metallurgical recovery were 30.95%, 54.12% and 40.58%, respectively. The results of the chemical assay showed 3.78 $\%Al_2O_3$ and 14.27% SiO_2. The results of the chemical composition of $\%Al_2O_3$ and $\%SiO_2$ in the tailings sample from the magnetic separator were 7.54% and 33.11%, respectively.

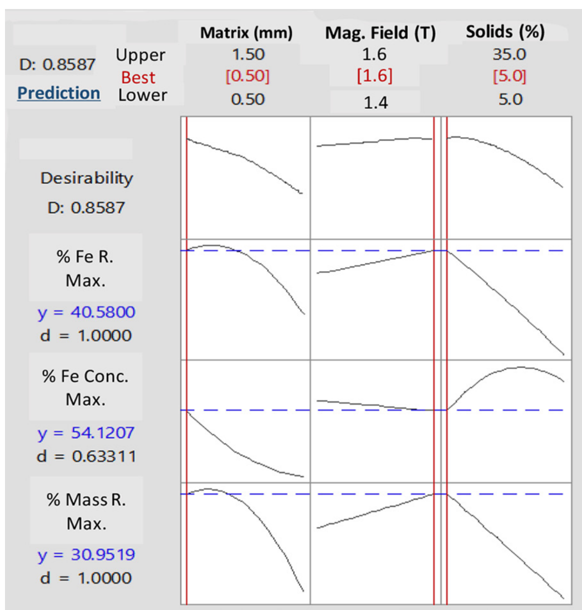

Figure 2 - Optimization graph for tests using WHIMS (Route 1).

3.2.2 Route 2

Considering the optimized parameters obtained from the factorial experimental design performed on Route 1 and the dispersion stage using the sodium silicate with the dosage at 500 g/t and at pH 11, before the magnetic separation, it was possible to reach a mass recovery, iron content in the magnetic concentrate and metallurgical recovery of 32.16%, 58.72% and 50.90%, respectively. Using this dispersion step before concentration, it is possible to observe an increase for the recovery of iron in relation to Route 1.

A considerable partition of particles above 20 µm migrating to the magnetic separator tailings was observed, probably attributed to quartz (Figure 3). The particles below 10 µm found in the magnetic desliming tailings can mainly be attributed to clay minerals containing alumina, which also migrates to the tailings. The results of the chemical composition for $\%Al_2O_3$ and $\%SiO_2$ of the magnetic concentrate were 2.21%

and 10.28%, respectively, while the results of the chemical composition for $\%Al_2O_3$ and $\%SiO_2$ of the magnetic tailing was 6.63% and 48.15%, respectively. The addition of the dispersing reagent allows the removal of the alumina and silica which were in the desliming tailing sample and directing them to the magnetic desliming tailings.

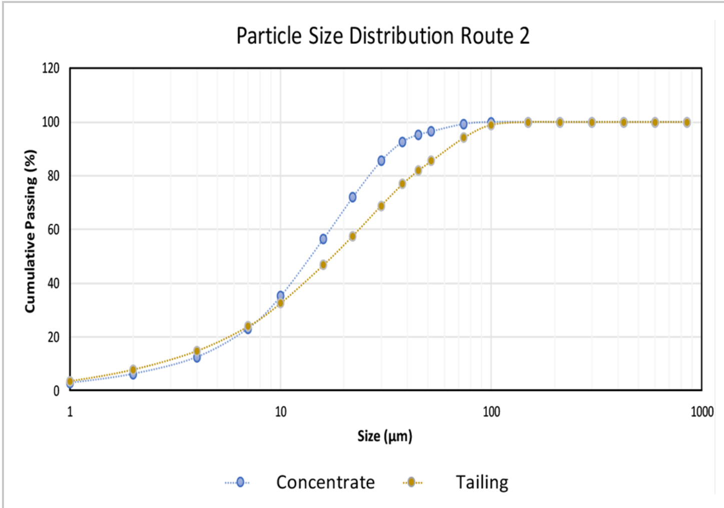

Figure 3 - Particle size distribution of the products obtained in the Route 2 tests.

The benefit of adding dispersant was justified by studying the electrical charges involved in the system. For this purpose, zeta potential measurements (ZP) of the major minerals in the tailings were carried out, in the presence of sodium silicate as a function of pH. As shown in Figure 4, it is observed that the presence of sodium silicate increases the magnitude of the zeta potential of quartz (that which was measured in the absence of sodium silicate was around 45mV in the studied pH range). The results found are in accordance with the DLVO theory, which predicts greater dispersion in conditions of higher modules of zeta potential. Consequently, the dispersion of quartz favors the dispersion of the system as a whole, thus favoring selectivity in the magnetic separation, since the dispersion inhibits the dragging of quartz particles in the flow of the magnetic particles. It is important to note that in the pH range between 9 and 11, sodium silicate prevails in the forms $[SiO(OH)^{3-}]$ and $[SiO_2(OH)_2^{2-}]$ (Marinakis & Shergold, 1985). Considering that these species have a negative charge and that the zeta potential of quartz is negative, the results suggest that sodium silicate is adsorbed by a chemical mechanism on the surface of the quartz, since the zeta potential of mineral becomes even more negative in presence of the reagent.

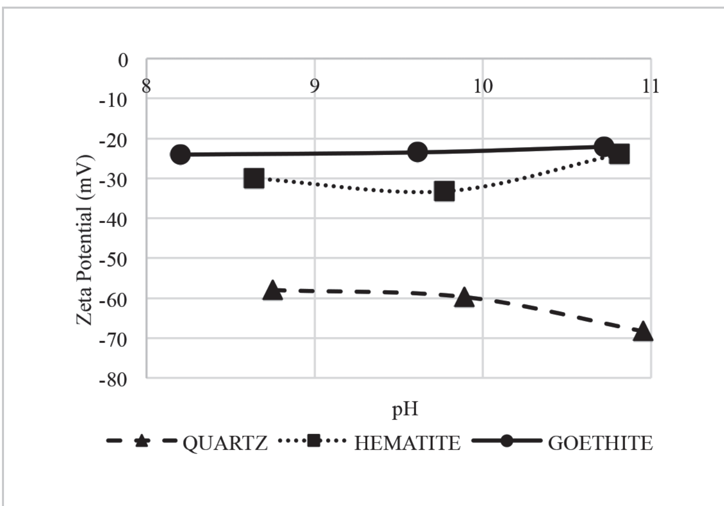

Figure 4 - Zeta potential of quartz, hematite and goethite, in the presence of sodium silicate, as a function of pH.

3.2.3 Route 3

The additional desliming step, before the magnetic concentration, improved the grade of Fe in the concentrate, but the overall recoveries values were lower than those obtained in the previous routes (Figure 5). The additional desliming step contributed to the cleaning of the material by reducing amount of alumina fed to the magnetic separator. In addition to the dispersion effect, the alumina content was around 2.43% representing a reduction of almost 60% of alumina contained in the desliming tailings under study. The silica content in the desliming tailing underflow product was 41.05%. This increase in the silica content in the magnetic separator feed can be attributed, mainly, to the quartz of greater granulation as identified in the QEMSCAN analyses (Table 1).

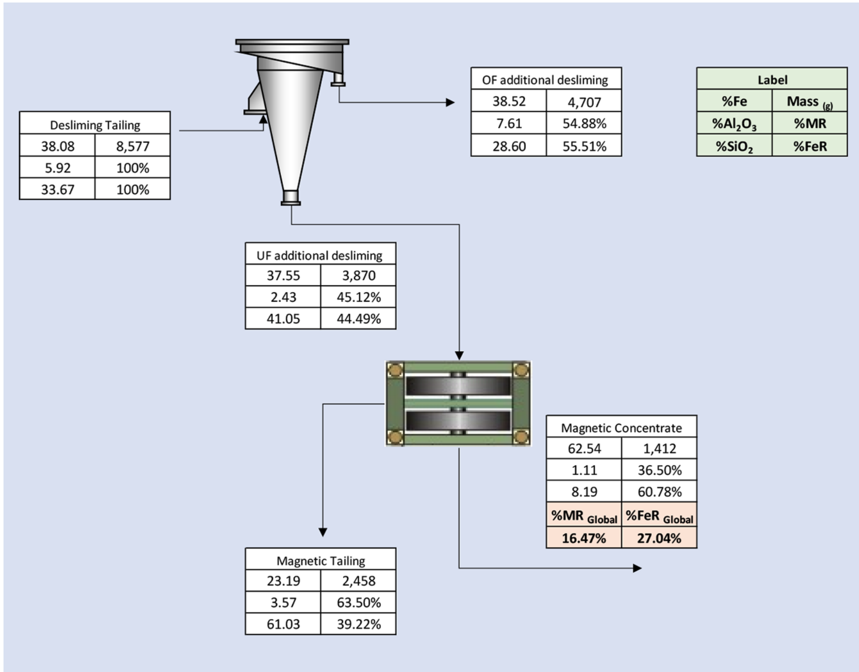

Figure 5 - Metallurgical balance Route 3.

The hydrocyclone partition was also distributed for this route. Plitt's equation was used to model the curve. The d_{50} of the additional desliming was 19 µm and 17 µm, respectively, for the experimental and modeled result. Most of the particles smaller than 10 µm were sent to the overflow of the additional desliming stage (Figure 6). The additional desliming step works very well to remove clay minerals, improving the efficiency of the magnetic separation. However, the loss of hematite in the fraction less than 10 µm is a negative consequence.

The results of the chemical composition of %Fe, %Al_2O_3 and %SiO_2 in the sample of the generated concentrate were 62.54%, 1.11% and 8.19%, respectively, while the chemical composition of %Fe, %Al_2O_3 and %SiO_2 in the magnetic desliming tailings were 23.19%, 3.57% and 61.03%, respectively.

When using a hydrocyclone, the additional desliming step removed a much larger fraction of particles smaller than 10 µm, analyzing the particle size distribution graphs of routes 2 and 3, which show the percentage of particles smaller than 10 µm in the magnetic separator products. The additional desliming contributed significantly to the removal of clay minerals before feeding into the magnetic separator, and also a considerable percentage of the mineral species, carrying iron, which are below this granulometry.

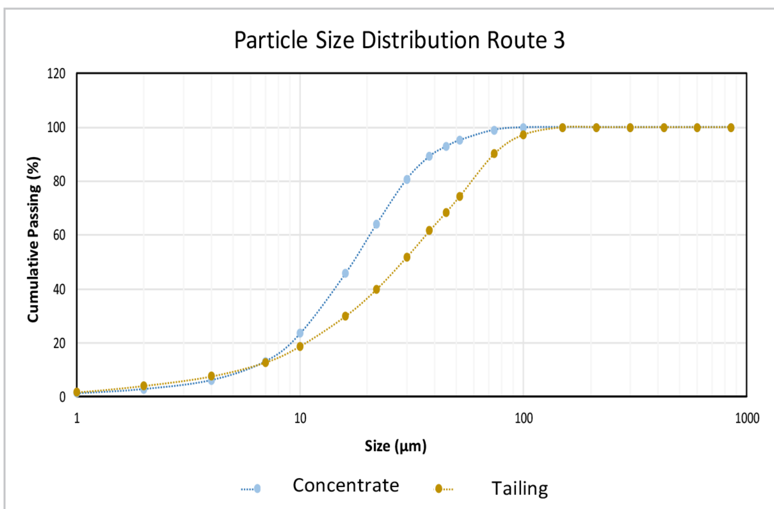

Figure 6 - Particle size distribution of the products obtained in the Route 3 tests.

3.2.4 Route 4

Considering the tests using the VPHGMS, it was possible to obtain 45.76%, 57.57% and 65.25% for mass recovery, iron content in the magnetic concentrate and iron recovery, respectively.

The particle size distribution of the products obtained from the Route 4 is shown in Figure 7. As expected, the behavior was also quite similar to that of the previous routes, presenting a granulometry for the rejection of the tailings from the magnetic separator for the range coarser than 10µm, compared to the concentrate of the magnetic separator, and finer for the range less than 10µm, also compared to the concentrate of the magnetic separator.

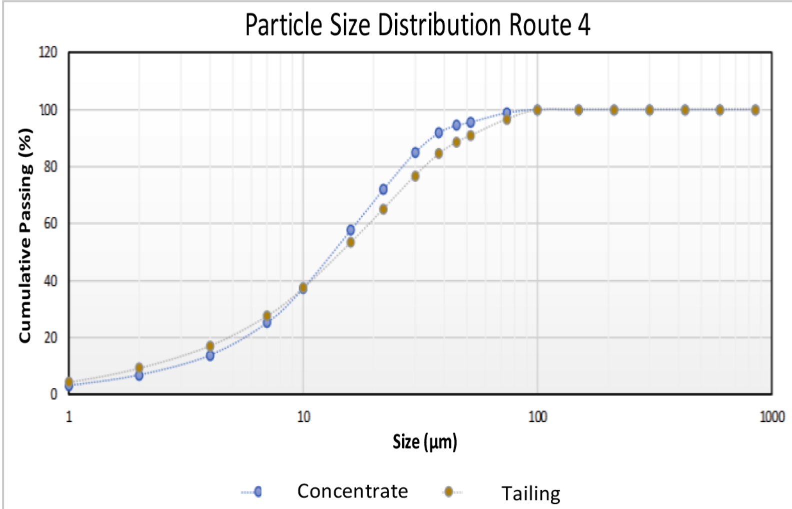

Figure 7 - Particle size distribution of the products obtained in the Route 4 tests.

The results of the chemical composition of %Al_2O_3 and %SiO_2 in the concentrate were 3.70% and 9.60%. The results of the chemical composition of %Al_2O_3 and %SiO_2 in the tailings from the magnetic separator were 9.49% and 45.39 %, respectively.

3.2.5 WHIMS (Wet Hight Intensity Magnetic Separation) x VPHGMS (Vertically Pulsating Hight Gradient Magnetic Separation)

By performing the comparative analysis between the pilot scale equipment, using metallurgical recovery as an evaluation parameter, the VPHGMS provides better results. It was possible to achieve 62.25% metallurgical recovery. The best WHIMS route (Route 02) provided 50.90% metallurgical recovery. All tests provided a high-quality pre-concentrate.

Another factor to note is the percentage of particles smaller than 10 µm in the concentrate. Table 3 shows us the summary of these results. For route 1, considering the sample as it is, it is noted that there is a greater proportion of ultrafine material (-10 um). When adding a dispersing reagent (route 2) this amount decreases in the obtained concentrate due to the positive actions of the reagent in making the removal of ultrafines more efficient (the alumina content, associated with the presence of ultrafines, drops). For route 3, in addition to the addition of dispersant, there is an additional desliming step, causing a greater reduction of alumina for the obtained concentrate, and also a decrease in the percentage of material below 10 µm.

Table 3 - Comparison of results obtained between WHIMS x VPHGMS.

Mag. Sep.	Route	%Fe Conc.	%Fe Tail	%SO_2 Conc.	%Al_2O_3 Con_c	%Mass. Rec.	%Fe Rec.	-10 µm (%) Conc.
WHIMS	1	54.12	30.89	14.27	3.78	30.95	40.58	43
	2	58.72	28.30	10.28	2.21	32.16	50.90	37
	3	62.54	23.19	8.19	1.11	16.47	27.04	23
VRPHGMS	4	57.57	21.64	9.60	3.70	45.76	62.25	39

For route 4, only dispersant reagent was used, as in route 2. However, the percentage of alumina associated with the final concentrate was higher than that associated with route 2 (Figure 8).

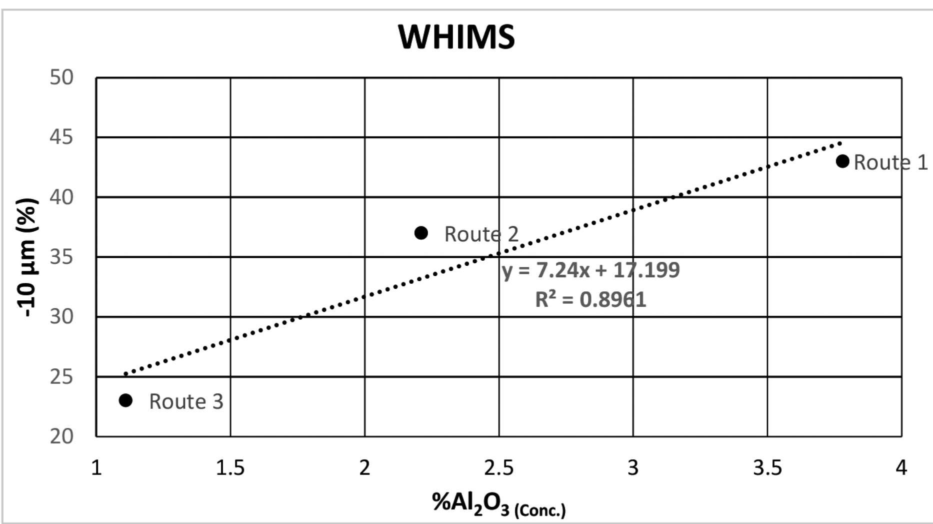

Figure 8 - Percentage of Al_2O_3 in the fraction below 10 µm of the concentration.

4. Conclusions

The slime iron ore under study has an iron content of 38%, 33.67% of SiO_2 and 5.92% of Al_2O_3 . It is composed largely of hematite, goethite, quartz, muscovite, kaolinite and gibbsite. Hematite and clay minerals are the predominant mineral species with up to 20 µm granulation. Almost 60% of quartz is also below 20 µm and about 40% is between 20 µm and 80 µm. The magnetic separation applied to concentration of desliming tailings using high-intensity magnetic separators was proven to be an advantageous technique. The best results were obtained using the VPHGMS model Slon® 100, with an average iron grade of 67% in the concentrate. Saving calculations show that around 540 thousand tons of concentrate can be incorporated into production, that is, not being discarded, not generating risks and losses. The tests carried out on the pilot scale were important for an evaluation of a possible commissioning and development of technology, as they allow an increase in the adherent and more adequate scale, with capacity of the industrial environment.

Acknowledgments

This work was supported by CNPQ, FAPEMIG, UFOP and Anglo American.

References

AROL, A. I.; AYDOGAN, A. Recovery enhancement of magnetite fines in magnetic separation. ***Colloids and Surfaces A***: Physiochemical and Engineering Aspects, v. 232, p. 151-154, 2004.

CHEN, L.; XIONG, D.; HUANG, H. Pulsating high-gradient magnetic separation of fine hematite from tailings. ***Minerals & Metallurgical Processing,*** v. 26, p. 163-168, 2009.

DAUCE, P. D.; CASTRO, G. B.; LIMA, M. M. F.; LIMA, R. M. F. Characterisation and magnetic concentration of an iron ore tailings. ***Journal of Materials Research and Technology,*** v. 8, n. 1, p. 1052-1059, 2019.

DWORZANOWSKI, M. Maximizing hematite recovery within a fine and wide particle-size distribution using wet high-intensity magnetic separation. ***Journal of the Southern African Institute of Mining and Metallurgy,*** v. 114, p. 559-567, 2014.

FORSSBERG, K. S.; KOSTKEVICIUS, N. R. Comparative pilot scale test with wet high intensity magnetic separation. ***Erzmetall,*** v. 35, n. 6, p. 285-293, 1982.

JENA, S. K.; SAHOO, H.; RATH, S. S.; RAO, D. S.; DAS, S. K.; DAS, B. Characterization and processing of iron ore slimes for recovery of iron values. ***Mineral Processing and Extractive Metallurgy Review,*** v. 36, n. 3, p. 174–82, 2015.

LI, C.; SUN, H.; BAI, J.; LI, L. Innovative methodology for comprehensive utilization of iron ore tailings: part 1. The recovery of iron from iron ore tailings using magnetic separation after magnetizing roasting. ***Journal Hazardous Materials,*** v. 174, p. 71-77, 2010.

LU, S.; PUGH, R. J.; FORSSBERG, E. Magnetic co-aggregation and combined aggregation. In: LU, S.; PUGH, R. J.; FORSSBERG, E. ***Interfacial separation of particles. Amsterdam: Elsevier,*** 2005. cap. 9, p. 497-516. (Studies in Interface Science, v. 20).

MARINAKIS, K. I.; SHERGOLD, H. L. Influence of sodium silicate addition on the adsorption of oleic acid by fluorite, calcite and barite. ***International Journal of Mineral Processing,*** v. 14, p. 177-193, 1985.

MARTINEZ, H. A. G.; SHAOXIAN, S.; VALDIVIESO, A. L. In situ observation of quartz particles entrained into magnetite coagulates in a uniform magnetic field. ***Minerals Engineering,*** v. 24, n. 8, p. 963-966, 2011.

MOHANTY, S.; NAYAK, B.; KONAR, J. Beneficiation of high-alumina bearing iron-ore slime: a case study from Eastern India. ***Mineral Processing and Extractive Metallurgy Review,*** v. 38, n. 6, p.403–410, 2017.

OZCAN, O.; CELIK, I. B. Beneficiation routes for upgrading iron ore tailings with a teetered bed separator. ***Separation Science and Technology,*** v. 51, n. 17, p.2844–2855, 2016.

RIBEIRO, J. P.; RIBEIRO, C. H. T.; PINTO, P. F.; ROCHA, R. B. D. The challenge to scavenge iron from tailings produced by flotation. A new approach: The super-WHIMS & the BigFLUX magnetic matrix. ***REM-International Engineering Journal,*** v. 70, n.3, p. 357–63, 2017.

ROCHA, R. B.; REIS, E. L.; RIBEIRO, J. P. Wet High-Intensity Magnetic Separators (WHIMS) for recovering iron from tailings deposited in dams. ***Mineral Processing and Extractive Metallurgy Review,*** v. 42, n. 1, p.17-23, 2019.

ROY, S.; DAS, A. Recovery of valuables from low-grade iron ore slime and reduction of waste volume by physical processing. ***Particulate Science and Technology,*** v. 31, p.256-263, 2013.

SILVA, M. B.; LUZ, J. A. M. Magnetic scavenging of ultrafine hematite from itabirites. ***REM-International Engineering Journal,*** v. 66, n.4, p.499–505, 2013.

SONG, S.; LU, S.; VALDIVIESO, A. L. Magnetic separation of hematite and limonite fine as hydrophobic flocs from iron ores. ***Minerals Engineering,*** v. 15, n. 6, p. 415-422, 2002.

SVOBODA, J.; FUJITA, T. Recent developments in magnetic methods of material separation. ***Minerals Engineering,*** v. 16, n. 9, p.785–792, 2003.

WANG, Y.; FORSSBERG, E. The recovery of hematite and chromite fines and ultrafines by wet magnetic methods. ***Minerals and Metallurgical Processing,*** v. 11, n.2, p. 87-96, 1994.

WOLFF, A. P.; COSTA, G. M.; DUTRA, F. C. A comparative study of ultra-fine iron ore tailings from Brazil. ***Mineral Processing and Extractive Metallurgy Review,*** v. 32, n. 1, p. 47–59, 2010.

YANGA, H.; JING, L.; ZHANG, B. Recovery of iron from vanadium tailings with coal-based direct reduction followed by magnetic separation. ***Journal of Hazardous Materials,*** v. 185, n. 2-3, p. 1405-1411, 2011.

ZENG, W.; DAHNE, X. The latest application of SLon vertical ring and pulsating high gradient magnetic separator. ***Minerals Engineering,*** v. 16, n. 6, p.563-565, 2003.

Received: 9 August 2020 - Accepted: 2 February 2022.